RSC Advances

ROYAL SOCIETY OF CHEMISTRY

www.rsc.org/advances

A table of contents entry:

The excellent antiwear performance of a-C/WC coating in PAO+ZDDP achieved by the forming tribofilms and the tribochemical products.

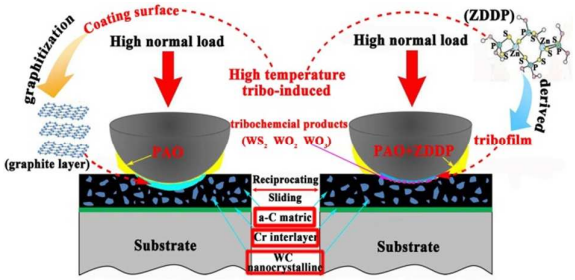

Study of tribological mechanisms of carbon-based coatings in antiwear additive containing lubricants under high temperature

Siming Ren[a], Shaoxian Zheng[a], Jibin Pu[b*], Zhibin Lu[b], Guangan Zhang[b]

[a]School of Mechatronic Engineering, Lanzhou Jiaotong University, Lanzhou 730000, PR China

[b]State Key Laboratory of Solid Lubrication, Lanzhou Institute of Chemical Physics, C hinese Academy of Science, Lanzhou 730000, PR China

Abstract

With the development of low-emission and low-consumption engines, diamond-like carbon (DLC) coatings have been considered as promising surface coatings of engine parts in terms of friction and wear performance. However, the performance of DLC-coated parts depends on the compatibility and interaction between coating and lubricant additives. To obtain high-performance coatings in the engine environment, the tribological behaviors of non-doped and metal-doped carbon-based coatings (a-C and a-C/WC, respectively) were studied systematically in poly-alpha-olefin (PAO) oil at 180 °C (operating temperature of engine oil) with and without antiwear additive zinc dialkyldithiophosphate (ZDDP) under various applied loads. Energy dispersive X-ray spectroscopy, Raman spectroscopy, and X-ray photoelectron spectroscopy were performed on a friction surface to understand tribological mechanisms. Results showed that ZDDP-derived tribofilms were able to suppress the surface graphitization of carbon-based coatings. The combination of ZDDP-derived tribofilms and tribochemical products WS_2/WO_2, which formed under

* *E-mail: nano@licp.cas.cn; Fax: +86-09318277088; Tel: +86-09314968117*

the joint actions of heat and contract pressure, led to improved tribological behavior of a-C/WC coating in PAO with ZDDP additive.

1. Introduction

Diamond-like carbon (DLC) coatings dominated by sp^2 sites, which have high load bearing capability, good adhesive strength, and excellent tribological properties, have been used as surface coatings of engine parts, such as piston rings.[1-3] High requirements for DLC coatings have been put forward with the development of low-emission and low-consumption engines. Doping is an effective means to improve the tribological properties of DLC coatings under dry sliding.[4] Therefore, more research on the tribological performance of doped carbon-based coatings under engine oils with lubricant additives are still needed for further operation of these coatings under the harsh engine environment, such as high temperature/load.

In the past, a great deal of research has been performed to investigate the tribological performance of DLC coatings under base oil condition.[5,6] Vengudusamy *et al.* reported the friction and wear behavior of four types of DLC coatings in base oil.[4] They found that tetrahedral amorphous carbon (ta-C) coating provides lower boundary friction than the other types. W-DLC coating experiences more wear, whereas Si-DLC and hydrogenated DLC (HDLC) coatings show very little wear. However, these results could not explain the tribological behavior of the DLC coatings in the engine oil through the formulation of suitable additives. In the recent years, many researchers have evaluated the tribological performance of DLC coatings in lubricating oil with anti-wear (AW) and extreme pressure (EP) additives, including dialkyldithiophosphate (ZDDP).[7-20] Some reported the presence of ZDDP-derived tribofilms on DLC coatings,[7-9] and usually attributed the excellent wear protection of DLC coatings under boundary lubrication to the formation of tribofilms on the coating surface. Equey *et al.* used several techniques to analyse the surfaces following sliding on both DLC and steel (self-mated) systems.[17] They found tribofilms formation on both DLC and steel

surfaces under very low wear conditions in the absence of iron. Haque *et al.* also studied the influence of antiwear additive ZDDP on the friction and wear of non-doped carbon-based coating (a-C) against cast iron.[8] X-ray photoelectron spectroscopy (XPS) results suggest that antiwear additive ZDDP was decomposed under tribological contacts and formed tribofilms on both interacting surfaces.

Podgornik *et al.* found that sulfur-based EP additives can reduce the friction and wear of metal-doped DLC coating (such as W-DLC), whereas phosphorous-based AW additives only had a minor effect, and the increase in contact pressure or temperature accelerated the process of friction reduction.[15] They suggested that higher temperatures accelerated the formation of WS_2-containing tribofilms with higher sulfur content and consequently resulted in lower friction. However, great attention has been paid to the tribological behavior of DLC coatings in lubricating oils with anti-wear additive ZDDP at room temperature or less than 100 °C. The tribological mechanisms of doped carbon-based coatings under the operating temperature (180 °C) of the engine oil with ZDDP additive are not well-understood yet. In this work, the tribological properties of a-C and WC-doped carbon-based (a-C/WC) coatings in synthetic poly-alpha-olefin (PAO) base oil and PAO through the formulation of ZDDP were studied at the high temperature of 180 °C. Accordingly, this study aimed to obtain the optimum carbon-based coating applicable to harsh engine environments and to explore the tribological mechanisms of carbon-based coatings in high-temperature PAO oil with ZDDP additive.

2. Experimental details

2.1. Deposition and characterization of DLC coatings

High speed steel (GCr15), 30-mm diameter and 3-mm thickness, with a hardness of 25 HRC and a surface roughness (Ra) of 20 nm, were used as the substrate. The substrates were first cleaned ultrasonically in acetone and alcohol for 15 min, respectively, and then located in vacuum chamber were cleaned by Ar^+ ion sputtering for 10 min under

pulsed bias of -500 V. Prior to coating deposition, a Cr interlayer of approximately 0.2 μm in thickness was deposited on the high speed steel substrate to improve the adhesion between the carbon-based coatings and substrates. The a-C and a-C/WC coatings were separately deposited on Cr interlayer by magnetron sputtering of graphite and WC targets with 99.99 % purity for the same time under a substrate pulsed bias of -70 V. For deposition a-C/WC coating, the D.C. power of the graphite target was kept constant at 2500 W and the D.C. power of the WC target was varied for desirable composition (from 0 W to 400 W with a step of 80 W), where a-C coating was prepared at 0 W. Fig. 1 shows the cross-sectional images of the as-deposited a-C and a-C/WC coatings under optimal parameters. The thickness of Cr interlayer, a-C and a-C/WC layers are approximately 200, 2600 and 5200 nm, respectively. The mechanical properties for a-C and a-C/WC coatings, such as hardness and elastic modulus are provided in Table 1.

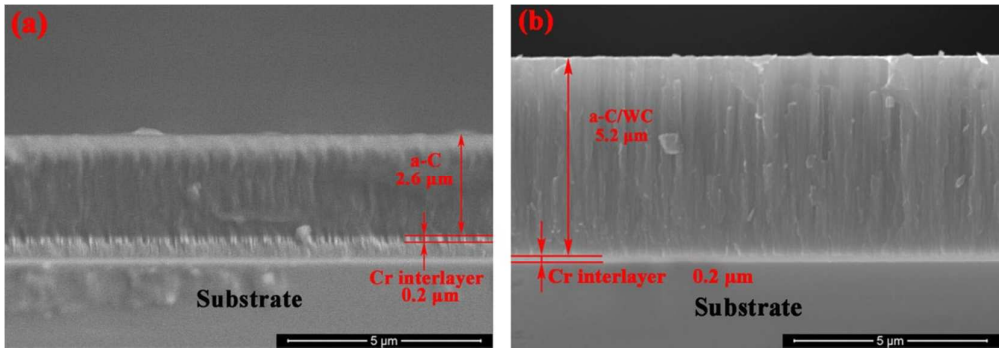

Fig. 1 Cross-sectional SEM images of the as-deposited (a) a-C and (b) a-C/WC coatings.

Table 1. Composition and mechanical properties of the carbon-based coatings.

Coating	Thickness (μm)	Roughness (R_q)	Composition (at. %)	Interal stress (GPa)	Hardness and modulus (GPa)
a-C	2.8	4.8	96.99 at% C, 3.01 at% O	-0.53	H: 17 GPa E: 200 GPa
a-C/WC	5.4	5.5	92.20 at% C, 4.85 at% W, 2.95 at% O	-0.32	H: 14.3 GPa E: 165 GPa

2.2. Friction and wear test

Tribological tests were performed on a commercially available reciprocating sliding friction and wear device (Optimol-SRV-IV). The tests were based on a ball-on-plate configuration, where a steel ball of 10-mm diameter with 710 HV hardness was loaded and rubbed against a carbon-based coating. The loads of 20, 60, 100, and 140 N were applied through a stationary loading system, and the corresponding initial maximum Hertzian contact pressure were about 1.2, 1.7, 2.0, and 2.3 GPa, respectively. The stroke was 2 mm and the frequency was 20 Hz, which provided a velocity of 0.08 m/s. A commercially available synthetic PAO was used as the base oil in this study. Anti-wear additive ZDDP was added to the PAO (labeled as PAO+ZDDP) with the aid of ultrasonication to obtain a formulated lubricating oil with an additive concentration of 3.0wt%. Two droplets of the base or formulated oil were spread on the coating surface before the mating steel ball was brought in contact. The contacts were pre-heated to 180 °C and the total sliding distance in each experiment was 144 m (sliding duration of 1800 s).

The loaded ball was rubbed against carbon-based coatings in lubricants with or without additives to analyse the effect of additive on tribological behavior of coatings.

After friction testing, the surface profile of wear track was measured using a D-100, KLΛ, Tencor surface profiler. The wear volume of each wear track was derived from three to five measurements to calculate the average value. The wear rates of the coatings were calculated from their wear volumes using the following equation:

$$K = V/SF \quad (1)$$

where V is the wear volume in mm^3, S is the total sliding distance in meter, and F is the normal load in newtons.

The corresponding lubrication regime can be approximately predicted according to the λ ratio in Eq. (2), where h_{min} corresponds to the minimum film thickness by the means of the well-known Hamrock–Dowson formula for isoviscous-elastic lubrication in Eq. (3),[21] and R'_q is the composite roughness evaluated by replacing the average R_q by the root mean squared roughness R'_q in Eq. (4), so defined:

$$\lambda = \frac{h_{\min}}{R'_q} \quad (2)$$

$$\frac{h_{min}}{R'} = 2.8\left(\frac{\eta\mu_e}{E'R'}\right)^{0.65}\left(\frac{W_y}{E'R'^2}\right)^{-0.21} \quad (3)$$

$$R'_q = \sqrt{R_{q1}^2 + R_{q2}^2} \quad (4)$$

Eq. (3) is appropriate for an equivalent ball-on-plane configuration in the quasi-static condition. The h_{min} is proportional to the effective radius (R'), the lubricant viscosity (η), the sliding velocity (μ_e), and inversely proportional to the average vertical load (W_y) and elasticmodulus (E'). Therein,

$$\frac{1}{R'} = \frac{1}{R_1} - \frac{1}{R_2} = \frac{R_2 - R_1}{R_1 R_2} \quad (5)$$

$$\frac{1}{E'} = \frac{1}{2}\left(\frac{1-\nu_1^2}{E_1} + \frac{1-\nu_2^2}{E_2}\right) \quad (6)$$

where R_1, E_1, ν_1 and R_2, E_2, ν_2 are the radii, Young's modulus and Poisson ratio of the ball and coating, respectively. According to the relevant parameters, h_{min} is figured out based on of Eq. (3), around 8.2, 6.6, 5.9, and 5.5 nm corresponding 20, 60, 100, and 140 N for a-C coating, around 8.8, 6.9, 6.2, and 5.8 nm corresponding 20, 60, 100, and

140 N for a-C/WC coating. Furthermore, the Eq. (2) gave the λ ratio between 0.26~0.42 which means that all tests is in the boundary lubrication regime.

2.3. General characterization

The nanohardness (*H*) and Young's modulus (*E*) of coatings was measured using a Nanoindenter II microprobe with a diamond Berkovich (three-sided pyramid) indenter tip and the indentation depth was about 10% of the coating thickness to minimize the substrate contribution. The coatings' internal stress was measured by measuring the substrate bending using a profilometer and the Stoney's equation. Wear tracks of balls and coatings were examined using scanning electron microscopes (SEM), energy dispersive X-ray analysis (EDX), Raman spectroscopy, and X-ray photoelectron spectroscopy (XPS). After the friction and wear measurements, the surface chemical composition were determined using scanning electron microscopy-energy dispersive X-ray spectroscopy (SEM-EDS) (Oxford IE250 Energy Dispersive Spectrometer, EDS) under 20 kV accelerating voltage with 10 nA beam current. The chemical states of elements were analyzed by a PHI-5702 multifunctional X-ray photoelectron spectroscope (XPS) made by American Institute of Physics Electronics Company using K-Alpha irradiation as the excitation source. The binding energies of the target elements were determined at a pass energy of 29.3 eV, with a resolution of about ±0.3 eV, using the binding energy of contaminated carbon (C1s: 284.8 eV) as the reference. The structural characteristics of carbon-based coatings before and after friction testing were measured using Raman spectroscopy equipped with a 532 nm argon ion laser from 200 to 2000 cm^{-1}. The samples were cleared ultrasonically in ethanol and acetone bathes to remove residual oil and contaminants before conducting the Raman spectroscopy. The worn coatings were analysed using Raman spectroscopy in two regions: within and outside the worn tracks.

3. Results and discussions

3.1. Friction and wear

Fig. 2 shows the average steady-state friction coefficient as a function of load. The friction coefficients of the two carbon-based coatings are presents a tendency that the friction coefficient decreases with increasing loads. The same phenomenon was already found in another study.[22] Furthermore, the addition of the anti-wear additive ZDDP to the base oil had a practically minor effect on the level of average friction coefficient at a fixed load value. Fig. 3 shows the evolution of friction as a function of time for the carbon-based coatings lubricated by PAO and PAO+ZDDP under the applied loads of 20 and 140 N, respectively. The run-in periods in both conditions were almost the same (~100 s) and primarily dominated by the coating surfaces' roughness at this stage (Table 1). The friction coefficients of a-C and a-C/WC coatings fluctuated under the base oil case (Figs. 3a and 3c). However, when PAO+ZDDP was used, the friction coefficients were more stable than that using base oil for the two carbon-based coatings (Figs. 3b and 3d). This is probably because ZDDP-derived tribofilms have the ability to digest small wear debris from the rubbed steel surfaces, which is an important feature for maintaining a stable friction coefficient and the long wear life of the components.[23]

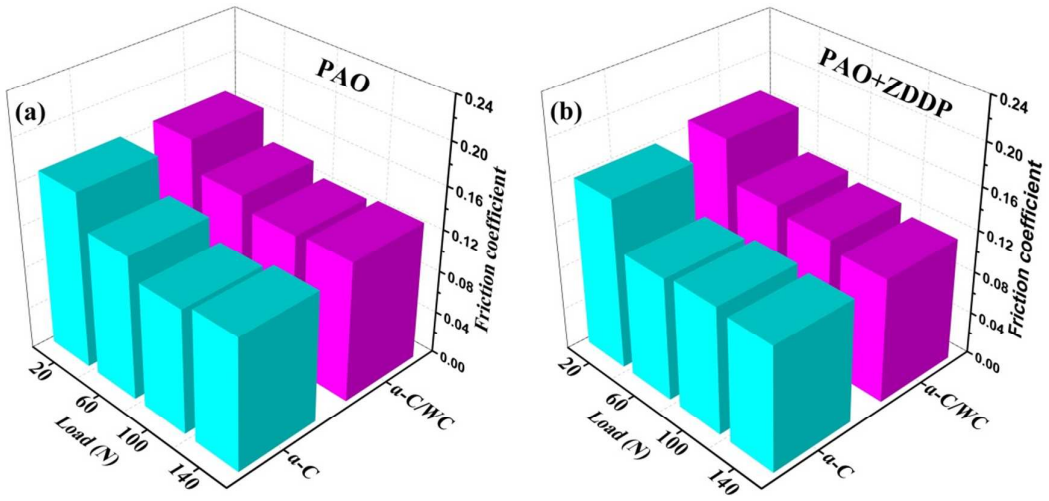

Fig. 2 The average steady-state friction coefficient of a-C and a-C/WC coating for 1800 s under applied loads of 20, 60, 100 and 140 N, respectively.

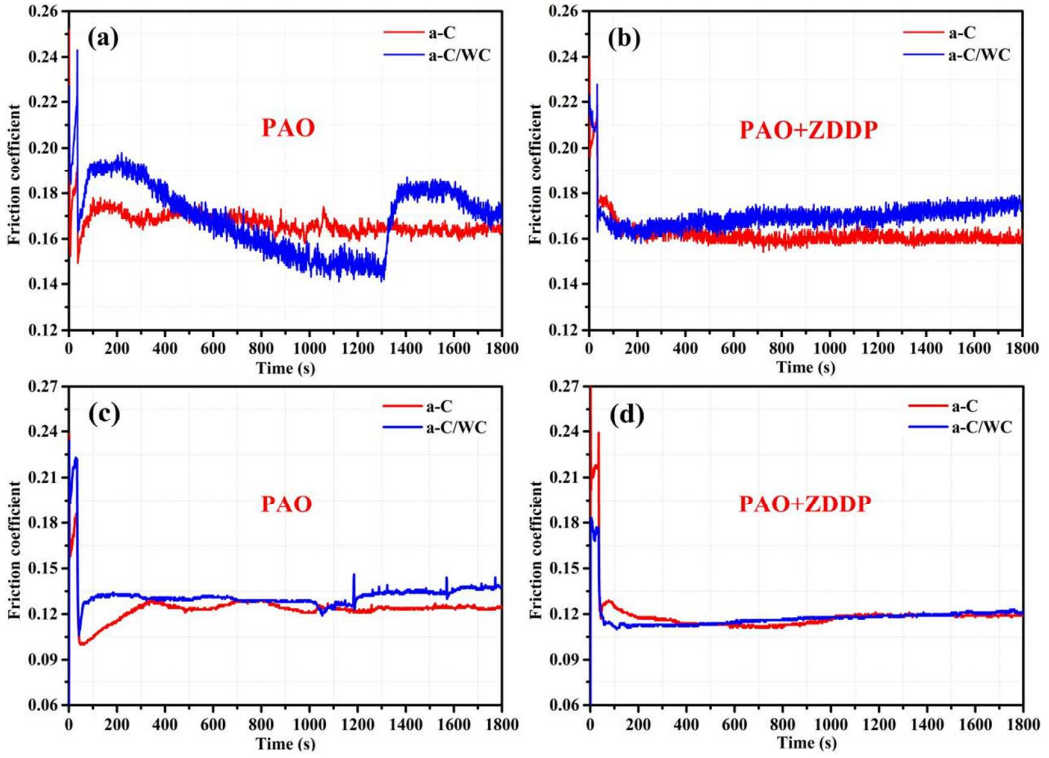

Fig. 3 Friction curves for a-C and a-C/WC coating: (a), (b) under applied load of 20 N; (c), (d) under applied load of 140 N.

The influence of the applied loads on the wear rate of a-C and a-C/WC coatings lubricated by PAO and PAO+ZDDP is shown in Fig. 4. The wear rates of the two coatings in both PAO and PAO+ZDDP lubricants increased with the increase of the applied load (except for the a-C/WC coating in PAO+ZDDP under 100 N). The non-doped carbon-based coating in PAO had a better wear resistance than the a-C/WC coating, especially under a high applied load (Fig. 4a), which was mainly attributed to the relative high hardness of a-C coating (Table 1). Moreover, the hard WC particles that formed on the friction interface intensified the abrasion of the a-C/WC coating under high applied loads. When ZDDP was added in PAO oil, the wear rates were reduced by one or two orders of magnitude under the same applied load. This effect was even more pronounced in the a-C/WC coating. As shown in Fig. 4b, the wear rate of a-C/WC coating in PAO+ZDDP was lower under the applied loads of 20, 60, and 100 N than that of the a-C coating. This was probably because a-C/WC coating was very helpful to the formation of ZDDP-derived tribofilms, which can prevent the direct contact between the friction pairs. To understand the effect of additive ZDDP to the two kinds of carbon-based coatings further, the corresponding ratio of the coatings volume loss in PAO+ZDDP to that in PAO under different applied loads is presented in Fig. 5. The volume loss ratio of both a-C and a-C/WC decreased first and increased afterward with the increase of applied load. The volume loss ratio of the a-C/WC coating was smaller than that of the a-C coating, which implied that a-C/WC had a better wear resistance in PAO+ZDDP than the a-C coating. In addition, a maximum volume loss ratio for a-C/WC coating was obtained under an applied load of 100 N. When the applied load further increased to 140 N, the wear protection of ZDDP lessened. This is probably because the ZDDP-derived tribofilms were scraped off easily under the applied high load and some hard grains generated in the tribochemical reactions between the a-C/WC coating and ZDDP under the high load resulted in a more severe abrasive wear. The arguments were proven by further experiments.

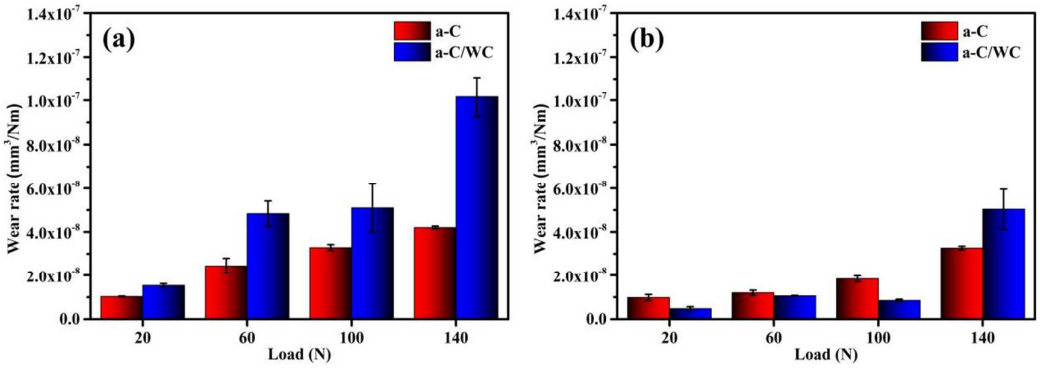

Fig. 4 The wear rates of the carbon-based coatings in (a) PAO, and (b) PAO+ZDDP.

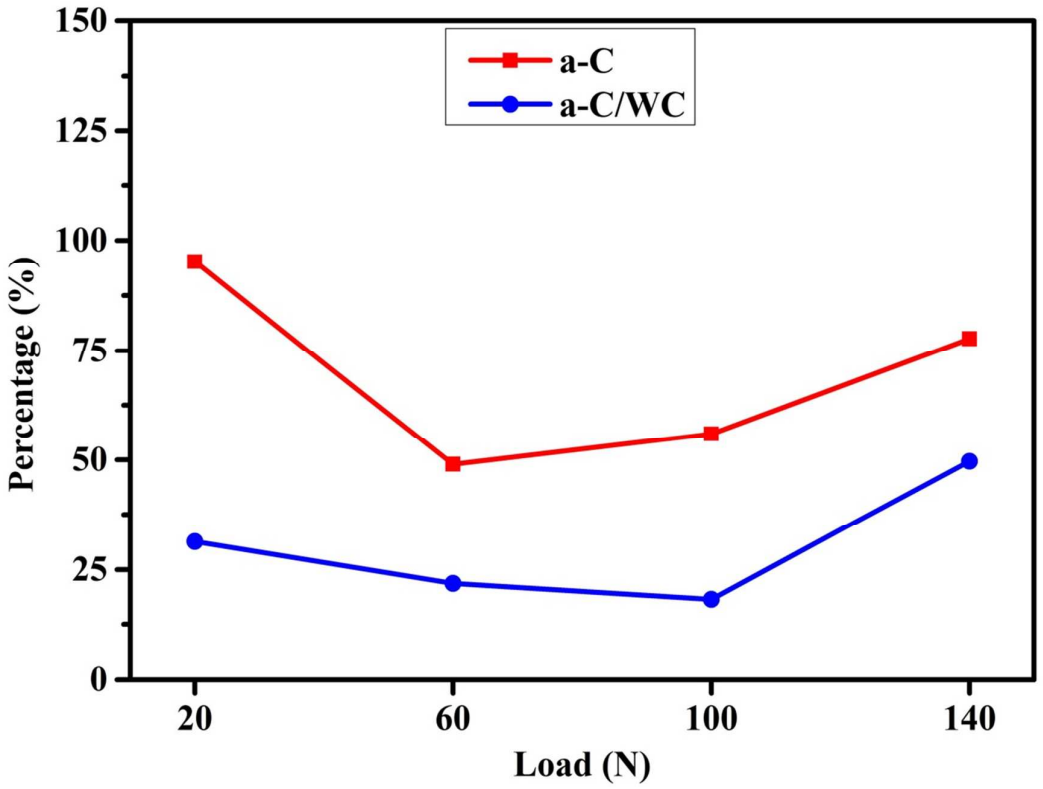

Fig. 5 Volume loss ratio (PAO+ZDDP/PAO, %) of the carbon-based coatings under different applied loads.

The surface SEM images and cross-section profiles of the wear tracks of the carbon-based coatings under an applied load of 100 N are shown in Fig. 6. The wear volume loss of the carbon-based coatings in PAO+ZDDP was very low compared with

that in PAO, and the wear track was shallow and narrow. Furthermore, the wear tracks in PAO showed deep plough and adhesion wear characteristics, whereas the wear tracks in PAO+ZDDP were very smooth and showed a featureless appearance. Thus, the friction reduction and wear resistance of the carbon-based coatings in PAO+ZDDP were dominated by the ZDDP-derived tribofilms or the tribochemical products.

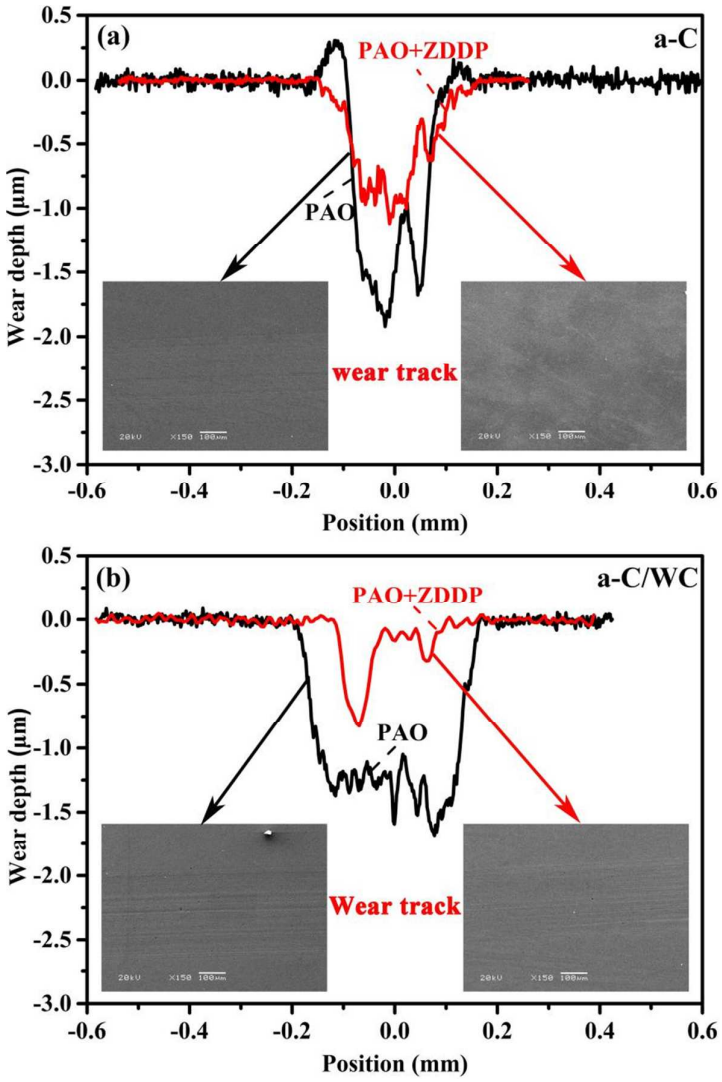

Fig. 6 SEM images and cross-section profiles of wear tracks of the carbon-based coatings in PAO and PAO+ZDDP under an applied load of 100 N.

3.2. ZDDP-derived tribofilm mechanism

The tribofilm formation mechanisms on steel surfaces have been detailed elsewhere.[24-26] As shown in Fig. 7, the characteristics of the wear scars on steel balls tested in PAO with and without additive ZDDP were quite different. When ZDDP was added to PAO, the wear scar area of the steel balls against the carbon-based coatings decreased significantly, and the contact surfaces of the mating steel balls were covered by continuous and compacted ZDDP-derived antiwear tribofilms, completely different from the wear scar of the steel ball couple in base oil PAO. The formed tribofilms could provide a protective effect, which sustains the relatively low wear volume loss of the carbon-based coatings in PAO+ZDDP. Furthermore, the tribofilm on the steel ball against a-C/WC was thicker and covered on a larger area, which could explain why the wear ratio of the a-C/WC coating was smaller than that of a-C in PAO+ZDDP under an applied load of 100 N.

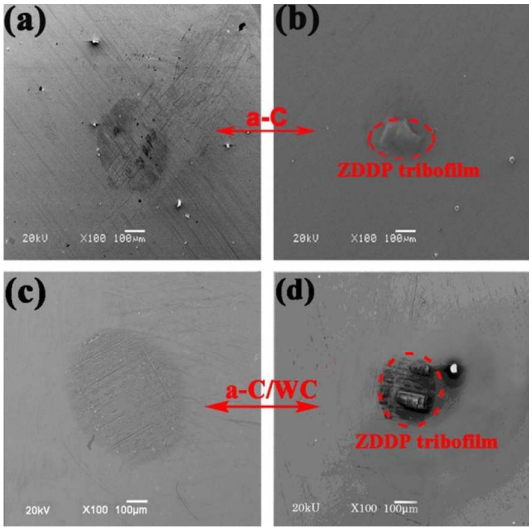

Fig. 7 SEM images of wear scar of steel ball (a), (b) against a-C coatings in PAO and PAO+ZDDP, (c), (d) against a-C/WC coatings in PAO and PAO+ZDDP under an applied load of 100 N.

The energy dispersive X-ray (EDX) elemental mapping of the wear scars of the steel balls against the carbon-based coatings tested in PAO and PAO+ZDDP under a

100 N load is shown in Fig. 8. A brighter area means a higher concentration of detected ion. The results indicated that the wear scars were covered with patches of oxidation layer, regardless of the ZDDP presence, whereas an apparent pad-like covering layer formed on the wear scar only in the presence of ZDDP. As indicated by the P, S and Zn mapping images in Figs. 8a and 8c, the covering layer was mainly dominated by the ZDDP-derived tribofilm rather than the carbon transfer film. Moreover, as shown in Figs. 8b and 8d, carbon or tungsten was enriched on the wear scar in the case of the base oil PAO. The coating material easily transferred to the mating steel ball and formed a carbon transfer film in the base oil PAO. However, the two kinds of elements were rarely detected on the steel ball wear scar in the PAO+ZDDP condition, which indicated that the transfer process could be suppressed by additive ZDDP. Following a sliding friction conducted at 100 N for the a-C/WC coating in PAO+ZDDP, wear debris were harvested from the resid. As shown in Fig. 9, the transmission electron micrograph (TEM) and selected area electron diffraction (SAED) of the wear debris indicated the formation of a large number of crystalline particles embedded within an amorphous matrix. According to the corresponding EDX, the debris was mainly made of ZDDP containing iron nano-particles. Some authors have reported that the wear debris containing iron and iron oxides have good wear resistance that protects the contact surface.[27,28]

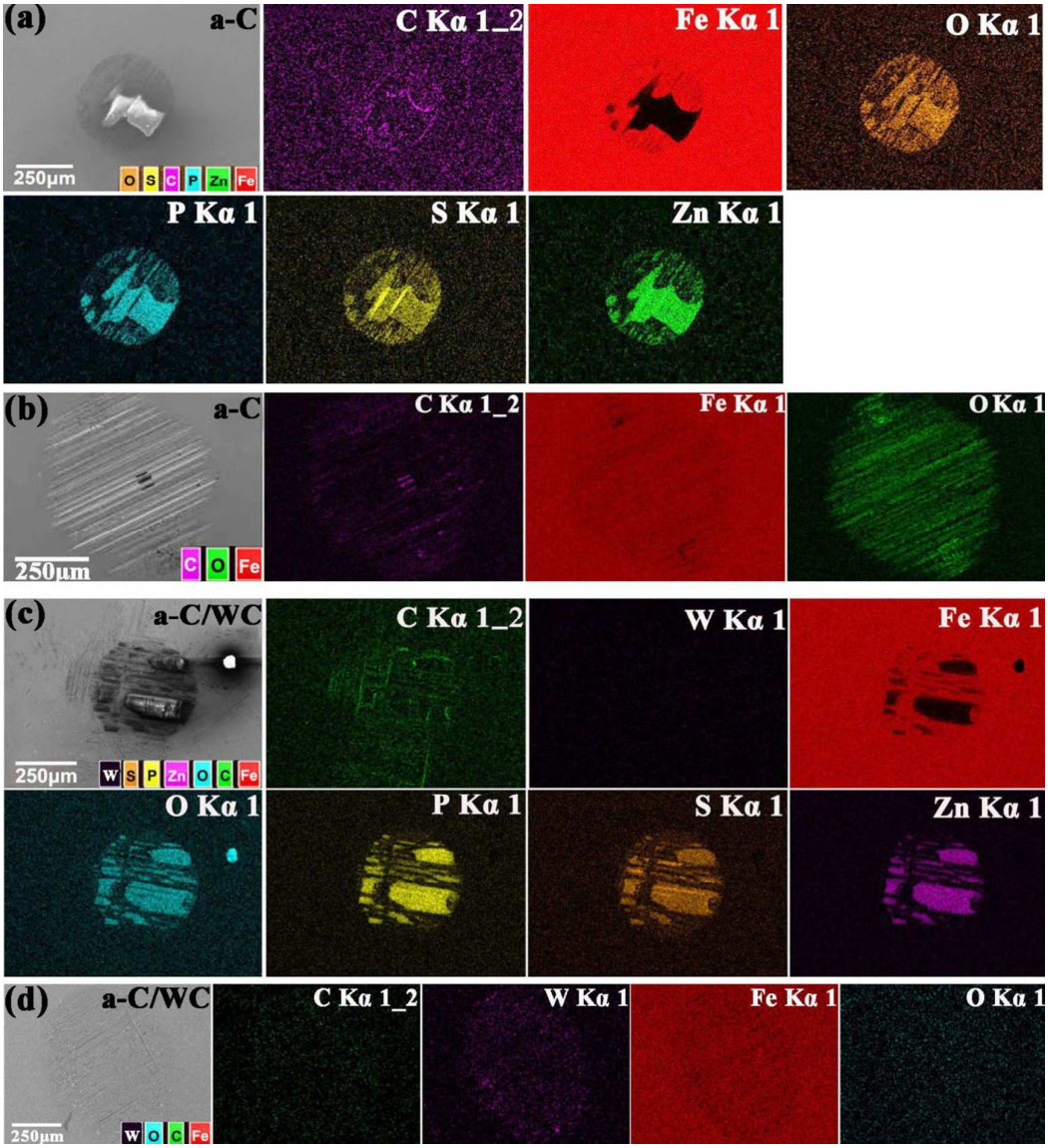

Fig. 8 Elemental distribution maps of wear scar on the steel balls sliding against (a) a-C and (c) a-C/WC coatings in the PAO+ZDDP, (b) a-C and (d) a-C/WC coating in the PAO under an applied load of 100 N.

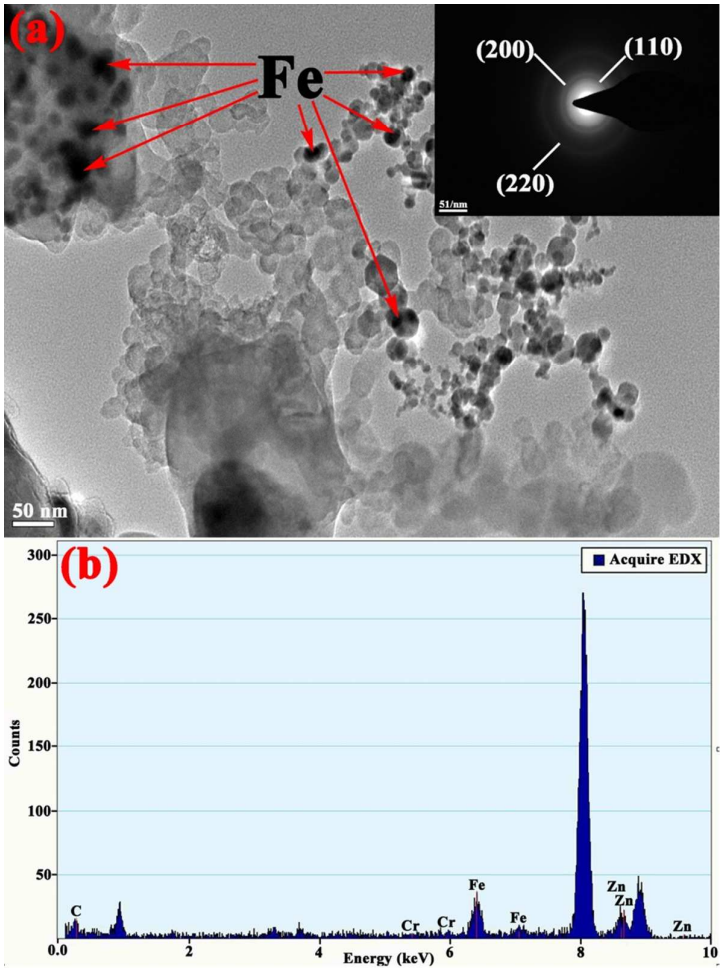

Fig. 9 (a) TEM, SAED, and (b) EDX of the wear debris from the test conducted at 100 N for a-C/WC coating in PAO+ZDDP.

XPS data of tribofilms of wear scar that formed on both carbon-based coatings and steel balls tested in PAO+ZDDP were obtained to determine the elemental chemical state of tribofilms. Fig. 10 shows the Zn 2p, S 2p, P 2p and O 1s XPS spectra of tribofilms that formed on the steel balls. The binding energies of Zn 2p (1022 eV), S 2p (164.4 eV), P 2p (134.2 eV) and O 1s (530.9 and 533.2 eV) peaks suggested that the tribofilms that formed on the steel ball were composed of ZDDP-derived ZnO/ZnS and zinc phosphate anti-wear species, which could provide wear protection.[7,8,29-31] Moreover, the intensities of these peaks for the steel ball against a-C/WC were stronger than that for the steel ball against a-C, which indicated

the formation of a thicker tribofilm on the steel ball against a-C/WC. Thus, metal doping tungsten elements can increase the surface activity of carbon-based coatings and promote the formation of tribofilm, and therefore results in good antiwear and friction reduction. More experiments were conducted to identify the effect of ZDDP on antiwear performance.

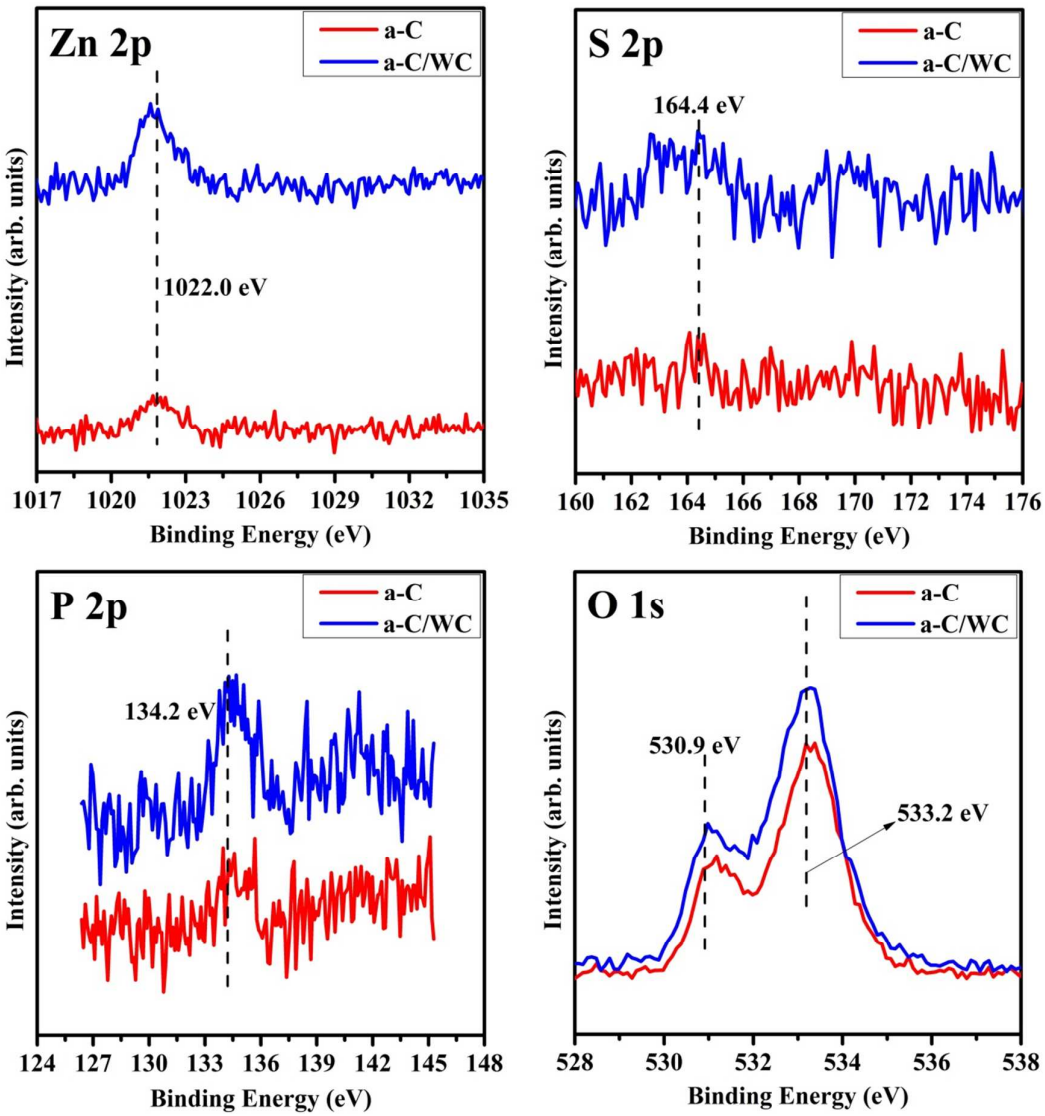

Fig. 10 XPS spectra of Zn 2p, S 2p, P 2p and O1s peaks obtained from the tribofilms formed by the PAO+ZDDP on the steel balls under the load of 100 N.

More than one mechanism operating in tribofilm formation may exist. Yin *et al.* described a mechanism in which ZDDP is concentrated in some of the metal surfaces and then interacts with the metal ions to form short or long chain zinc polyphosphates.[32] In Yin *et al.*'s mechanism, high temperature and load increase the rate of ZDDP decomposition and facilitate the formation of tribofilms. Fig. 11 shows the SEM images of the wear scars of the steel ball against the a-C/WC coating tested in PAO+ZDDP for all the applied loads. When the load was lowered to 20 N, less tribofilms were detected on the contact surface of the steel ball, and the protective effect was mainly ascribed to the formation of oil film by the mechanical and/or thermal action. These pad-like tribofilms on the mating steel ball surface increased with the applied loads. The tribofilms were completely covered on the worn scar when the load rose to 100 N. This is because the high contact pressure, along with the high energy input and thus the high potential, hastened the ZDDP-derived tribofilms formation and improved the friction reduction and antiwear properties. However, when the applied load rose to 140 N, the tribofilms were not observed clearly on the wear scar. This is because the removal rate of tribofilms from the contact surface was higher than its growth rate under excessive applied loads.[33] Thus, no antiwear performance from ZDDP existed.

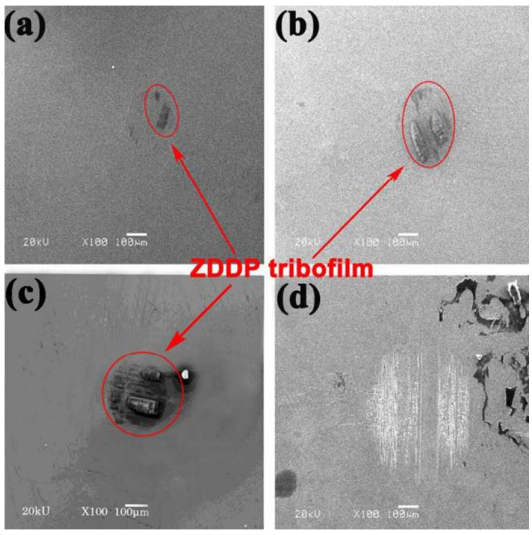

Fig. 11 SEM images of wear scar on the steel balls against a-C/WC coating tested in PAO+ZDDP under different loads: (a) 20 N, (b) 60 N, (c) 100 N, and (d) 140 N, respectively.

Fig. 12 shows the S 2p, P 2p and Zn 2p XPS spectra of the worn surfaces of the a-C/WC coatings tested in PAO+ZDDP under different applied loads. The results suggested that ZDDP was decomposed during the rubbing test and formed ZnS/ZnO and zinc phosphate corresponding to the binding energies of Zn 2p (1022.3 eV), S 2p (161.7 eV) and P 2p (133.8 eV).[7,8,29-31] Tribofilms formed on the contact surface of the coatings, further explaining the absence of carbon-based transfer film in the presence of ZDDP. Moreover, the content of S and Zn from ZDDP was larger under a high load than a low load, but the content of such elements decreased when the load increased to 140 N. This chemical change appears to agree well with the results in Fig. 11.

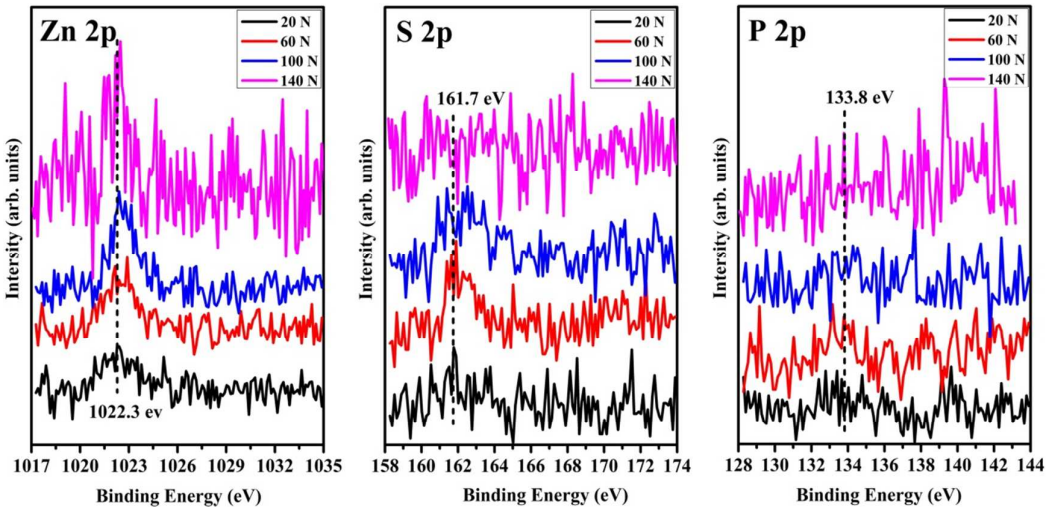

Fig. 12 XPS spectra of Zn 2p, S 2p and P 2p obtained from the worn surfaces of a-C/WC coating tested in PAO+ZDDP under different loads.

3.3. Graphitization mechanism of carbon-based coatings

Raman spectra of coating surfaces before and after rubbing in PAO and PAO+ZDDP were obtained to identify graphitization. Fig. 13 shows the Raman spectra obtained from the as-deposited coatings within and outside the wear tracks of coatings after sliding against steel balls under a load of 100 N. I_D/I_G ratio increased, and the G band peak within and outside the wear tracks of coatings shifted to a higher wave number after the rubbing tests. Temperature and/or contact pressure-induced graphitization of the carbon-based coatings may have occured.[34] In addition, the I_D/I_G ratio within the wear track of the carbon-based coatings tested in PAO was higher than that outside of the wear track, suggesting that the contact pressure was an important factor in inducing graphitization. The high wear rate in the base oil tests can be attributed to the formation of graphite layer on the contact surface. Particularly, the relatively soft graphite layers were more prone to mechanical damage and wear. However, for the coatings tested in the PAO+ZDDP, the intensity ratio I_D/I_G within the wear track dropped to a lower value than that of the base oil PAO, i.e., a lower degree in the presence of ZDDP. As proposed by Ferrari and Robertson,[35] the surface of the wear track tested in base oil suffered a higher graphitization than that lubricated in

PAO+ZDDP. According to Kalin,[36] the ZDDP-derived tribofilms that formed on the carbon-based coating surfaces reduced the peak contact stresses and resulted in a more homogeneous stress distribution at the friction interface, thus suppressing the tribo-induced graphitization under high load and temperature conditions. Meanwhile, compact and continuous tribofilms exerted a wear-protective effect at the interface.

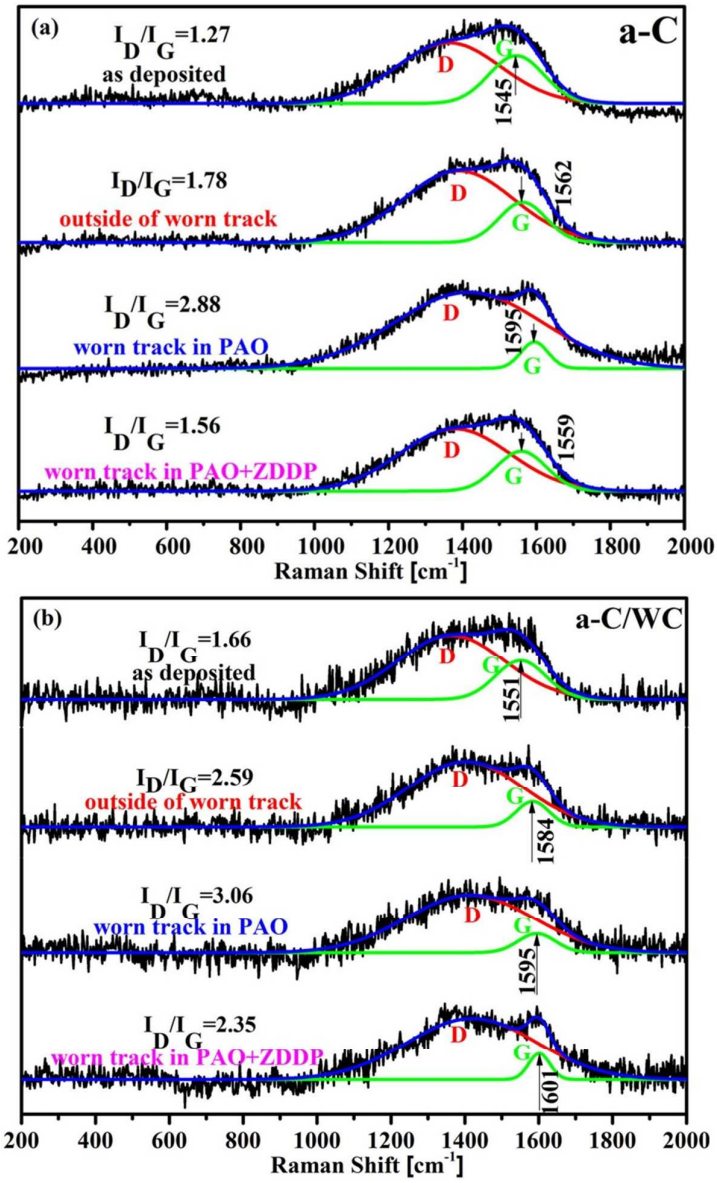

Fig. 13 Raman spectra from as deposited coatings, within and outside wear tracks of (a) a-C and (b) a-C/WC coatings tested in PAO and PAO+ZDDP at a load of 100 N.

3.4. Tribochemical reaction mechanism

The W 4f XPS spectra on the wear scar of the a-C/WC coating tested in PAO+ZDDP under applied loads of 100 and 140 N are shown in Fig. 14. The binding energies of W 4f (33.2, 34.2, 35.4, and 41.7 eV) corresponded with the WS_2/WO_x derived from the tribochemical reaction between a-C/WC coating and ZDDP.[29,37] Therefore, additive ZDDP could react with the metal doping phase under the combined action of high temperature and high applied load to form tribochemical products at the interface, which is in agreement with the results reported in a study of ZDDP at high temperature.[38] Thus, the formation of friction reduction or antiwear WS_2/WO_2 was also an important factor to the low wear rate of the a-C/WC coating under an applied load of 100 N (Fig. 14a). When the applied load increased to 140 N, the tribochemical reaction on the rubbing surface was governed by the formation of amounts of WO_3 (Fig. 14b). The formation of the hard particle (WO_3) accelerated the abrasive wear and resulted in the higher wear rate of the a-C/WC coating than that of the a-C coating.

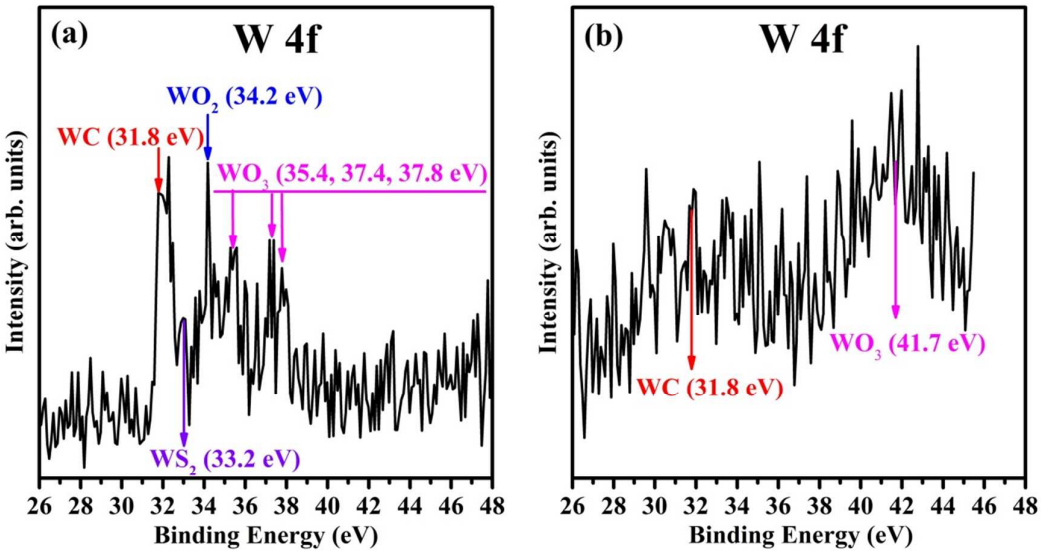

Fig. 14 The XPS spectra of W 4f obtained from wear scar of a-C/WC coating tested in PAO+ZDDP at (a) 100 N and (b) 140 N, respectively.

Fig. 15 shows the schematic of the friction mechanism for the a-C/WC coating during the reciprocating sliding in PAO and PAO+ZDDP. The excellent antiwear performance of the a-C/WC coating in PAO+ZDDP was dominated by two major effects. First, the EDX and XPS results provided direct evidence of the formation of ZDDP-derived tribofilms consisting of zinc phosphates and zinc sulfide/sulfates on the rubbing surface of the a-C/WC coating. In addition, the ZDDP-derived tribofilms was also formed on the a-C film although the tribofilm of a-C is thinner and smaller than that of a-C/WC, which suppressed graphitization and led to lower wear than PAO. The tribofilms at the interface can prevent the direct contact of tribo-pairs and suppress the graphitization under high load/temperature conditions, and result in good antiwear property (graphitization of the rubbing surfaces of carbon-based coatings in PAO contributed to friction reduction, but at the same time increased the wear). Moreover, the existence of doping tungsten elements increased the surface activity of the carbon-based coating, which was also beneficial to tribofilms formation and adsorption on the a-C/WC (Fig. 8). On the other hand, the products formed by tribochemical reaction between the metal doping phase in the a-C/WC coating and ZDDP under a certain range of load had good friction reduction and wear resistance, further reduced the wear, and prolonged lives of components. But for the a-C film, there are not the tribochemical products due to the lack of metal doping phase. Thus, the volume loss ratio (PAO+ZDDP/PAO, %) of the a-C coating was larger than that of the a-C/WC coating. However, the excessive contact pressure can destroy the dynamic equilibrium of ZDDP-derived tribofilms, leading to the impossibility of forming a continuous and compacted antiwear tribofilm on the rubbing surface. Additionally, for the a-C/WC tested in PAO+ZDDP, excessive contact pressure can promote the forming of hard WO_3, which increases the abrasive wear and worsen the tribological performance of the a-C/WC coating. However, the a-C coating has a relatively less change of wear in PAO+ZDDP because there is no hard WO_3 from tribochemical reaction.

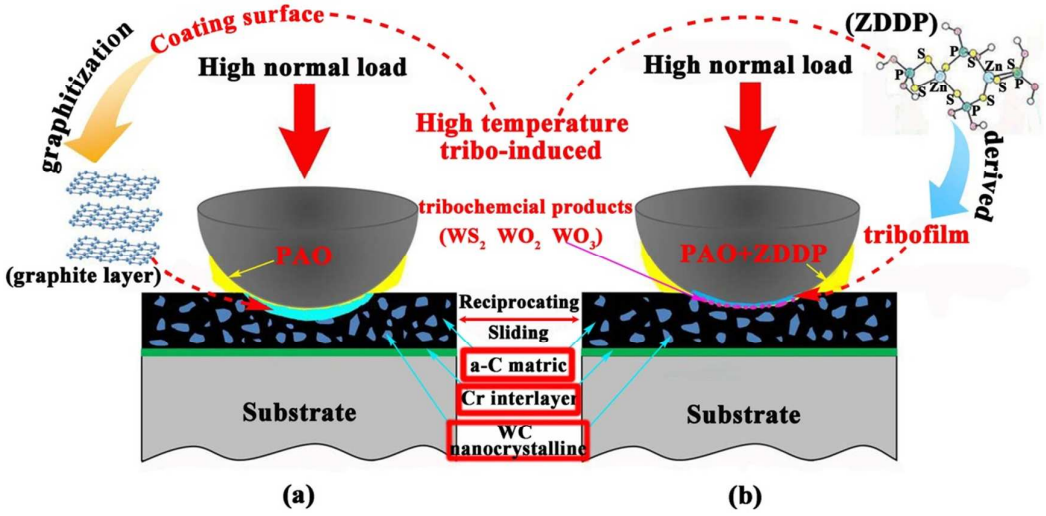

Fig.15 Schematic diagram of frictional mechanism for the a-C/WC coating lubricated with PAO and PAO+ZDDP.

4. Conclusions

The effect of contact pressure on the tribological performance of a-C and a-C/WC coatings was investigated in base oil PAO and PAO+ZDDP at 180 °C (operating temperature of engine lubricating oil). The following conclusions can be made.

1. Average steady-state friction coefficients slightly differed between a-C and a-C/WC coatings whether in PAO or PAO+ZDDP. However, when ZDDP was added to the base oil, the wear rate of the two carbon-based coatings decreased to more than one or two orders of magnitude higher than that in PAO. In particular, a-C/WC coating achieved better antiwear performance.

2. High temperature and contact pressure can induce the graphitization of the rubbing surface of carbon-based coatings in PAO during oscillating sliding. However, for the carbon-based coatings in PAO+ZDDP, ZDDP-derived tribofilm acted as a mechanically protective barrier that prevented tribo-induced graphitization. Therefore, the excellent antiwear performance of a-C/WC coating in PAO+ZDDP was due to the

formation of tribofilms and the tribochemical products WS_2/WO_2, which had good wear resistance and friction reduction that resulted in less wear loss than a-C coating.

Acknowledgements

The authors are grateful for financial support from the Program of the Light of the Chinese Academy of Sciences in China's Western Region (2013) and the National Natural Science Foundation of China (Grant No. 51305433)

References

1. A. Erdemir, Genesis of superlow friction and wear in diamondlike carbon films, *Tribol. Int.*, 2004, **37**, 1005-1012.
2. K. K. Mistry, A. Morina, A. Neville, A tribochemical evaluation of a WC–DLC coating in EP lubrication conditions, *Wear*, 2011, **271**, 1739-1744.
3. K. Topolovec-Miklozic, F. Lockwood, H. Spikes, Behaviour of boundary lubricating additives on DLC coatings, *Wear*, 2008, **265**, 1893-1901.
4. S. G. Zhou, L. P. Wang, Z. B. Lu, Q. Ding, S. C. Wang, R. J. K. Wood and Q. J. Xue, Tailoring microstructure and phase segregation for low friction carbon-based nanocomposite coatings, *J. Mater. Chem.*, 2012, **22**, 15782-15792.
5. H. Ronkainen, S. Varjus, K. Holmberg, Friction and wear properties in dry, water-and oil-lubricated DLC against alumina and DLC against steel contacts, *Wear*, 1998, **222**, 120-128.
6. B. Vengudusamy, R. A. Mufti, G. D. Lamb, J. H. Green and H. A. Spikes, Friction properties of DLC/DLC contacts in base oil, *Tribol. Int.*, 2011, **44**, 922-932.

7. T. Haque, A. Morina, A. Neville, R. Kapadia and S. Arrowsmith, Effect of oil additives on the durability of hydrogenated DLC coating under boundary lubrication conditions, *Wear*, 2009, **266**, 147-157.

8. T. Haque, A. Morina, A. Neville, Influence of friction modifier and antiwear additives on the tribological performance of a non-hydrogenated DLC coating, *Surf. Coat. Technol.*, 2010, **204**, 4001-4011.

9. H. A. Tasdemir, M. Wakayama, T. Tokoroyama, H. Kousaka, N. Umehara, Y. Mabuchi and T. Higuchi, Wear behaviour of tetrahedral amorphous diamond-like carbon (ta-C DLC) in additive containing lubricants, *Wear*, 2013, **307**, 1-9.

10. B. Podgornik, S. Jacobson, S. Hogmark, DLC coating of boundary lubricated components—advantages of coating one of the contact surfaces rather than both or none, *Tribol. Int.*, 2003, **36**, 843-849.

11. M. Kalin, J. Vižintin, J. Barriga, K. Vercammen, K. van. Acker and A. Arnšek, The effect of doping elements and oil additives on the tribological performance of boundary-lubricated DLC/DLC contacts, *Tribol. Lett.*, 2004, **17**, 679-688.

12. B. Podgornik, S. Jacobson, S. Hogmark, Influence of EP additive concentration on the tribological behaviour of DLC-coated steel surfaces, *Surf. Coat. Technol.*, 2005, **191**, 357-366.

13. B. Podgornik, D. Hren, J. Vižintin, S. Jacobson, N. Stavlid and S. Hogmark, Combination of DLC coatings and EP additives for improved tribological behaviour of boundary lubricated surfaces, *Wear*, 2006, **261**, 32-40.

14. A. Morina, A. Neville, M. Priest and J. H. Green, ZDDP and MoDTC interactions in boundary lubrication—the effect of temperature and ZDDP/MoDTC ratio, *Tribol. Int.*, 2006, **39**, 1545-1557.

15. B. Podgornik, M. Sedlaček, J. Vižintin, Influence of contact conditions on tribological behaviour of DLC coatings, *Surf. Coat. Technol.*, 2007, **202**, 1062-1066.

16. K. Topolovec-Miklozic, F. Lockwood, H. Spikes, Behaviour of boundary lubricating additives on DLC coatings, *Wear*, 2008, **265**, 1893-1901.

17. S. Equey, S. Roos, U. Mueller, R. Hauert, N. D. Spencer and R. Crockett, Tribofilm formation from ZnDTP on diamond-like carbon, *Wear*, 2008, **264**, 316-321.

18. M. Kalin, E. Roman, L. Ožbolt and J. Vižintin, Metal-doped (Ti, WC) diamond-like-carbon coatings: reactions with extreme-pressure oil additives under tribological and static conditions, *Thin Solid Films*, 2010, **518**, 4336-4344.

19. S. Kosarieh, A. Morina, E. Lainé, J. Flemming and A. Neville, Tribological performance and tribochemical processes in a DLC/steel system when lubricated in a fully formulated oil and base oil, *Surf. Coat. Technol.*, 2013, **217**, 1-12.

20. X. F. Liu, J. B. Pu, L. P. Wang and Q. J. Xue, Novel DLC/ionic liquid/graphene nanocomposite coatings towards high-vacuum related space applications, *J. Mater. Chem. A*, 2013, **1**, 3797-3809.

21. Z. M. Jin, D. Dowson, J. Fisher, Analysis of fluid film lubrication in artificial hip joint replacements with surfaces of high elastic modulus, *Proc. Inst. Mech. Eng. H J. Eng. Med*, 1997, **211**, 247-56.

22. B. Podgornik, J. Vižintin, S. Jacobson, and S. Hogmark, Tribological behaviour of WC/C coatings operating under different lubrication regimes, *Surf. Coat. Technol.*, 2004, **177**, 558–565.

23. J. M. Martin, T. Onodera, C. Minfray, F. Dassenoy and A. Miyamoto, The origin of anti-wear chemistry of ZDDP, *Faraday Discuss.*, 2012, **156**, 311-323.

24. V. Jaiswal, R. B. Rastogi, J. L. Maurya, P. Singh and A. K. Tewari, Quantum chemical calculation studies for interactions of antiwear lubricant additives with metal surfaces, *RSC Adv.*, 2014, **4**, 13438-13445.

25. M. Ratoi, V. B. Niste, H. Alghawel, Y. F. Suen and K. Nelson, The impact of organic friction modifiers on engine oil tribofilms, *RSC Adv.*, 2014, **4**, 4278-4285.

26. M. Ratoi, V. B. Niste and J. Zekonyte, WS_2 nanoparticles–potential replacement for ZDDP and friction modifier additives, *RSC Adv.*, 2014, **4**, 21238-21245.

27. J. M. Martin, J. L. Mansot, I. Berbezier and H. Dexpert, The nature and origin of wear particles from boundary lubrication with a zinc dialkyl dithiophosphate, *Wear*, 1984, **93**, 117-126.

28. G. Nehme, R. Mourhatch, P. B. Aswath, Effect of contact load and lubricant volume on the properties of tribofilms formed under boundary lubrication in a fully formulated oil under extreme load conditions, *Wear*, 2010, **268**, 1129-1147.

29. P. Forsberg, F. Gustavsson, V. Renman, A. Hieke and S. Jacobson, Performance of DLC coatings in heated commercial engine oils, *Wear*, 2013, **304**, 211-222.

30. J. Chastain and R. C. King (Eds.), *Handbook of X-ray photoelectron spectroscopy: a reference book of standard spectra for identification and interpretation of XPS data*, 1992, **261**, Eden Prairie, MN: Perkin-Elmer.

31. A. Morina, A. Neville, M. Priest and J. H. Green, ZDDP and MoDTC interactions and their effect on tribological performance–tribofilm characteristics and its evolution, *Tribol. Lett.*, 2006, **24**, 243-256.

32. Z. Yin, M. Kasrai, M. Fuller, G. M. Bancroft, K. Fyfe and K. H. Tan, Application of soft X-ray absorption spectroscopy in chemical characterization of antiwear films generated by ZDDP Part I: the effects of physical parameters, *Wear*, 1997, **202**, 172-191.

33. Y. C. Lin, H. So, Limitations on use of ZDDP as an antiwear additive in boundary lubrication, *Tribol. Int.*, 2004, **37**, 25-33.

34. J. Qian, C. Pantea, J. Huang, T. W. Zerda and Y. Zhao, Graphitization of diamond powders of different sizes at high pressure–high temperature, *Carbon*, 2004, **42**, 2691-2697.

35. A. C. Ferrari, J. Robertson, Interpretation of Raman spectra of disordered and amorphous carbon, *Phys. Rev. B*, 2000, **61**, 14095.

36. M. Kalin, E. Roman, J. Vižintin, The effect of temperature on the tribological mechanisms and reactivity of hydrogenated, amorphous diamond-like carbon coatings under oil-lubricated conditions, *Thin Solid Films*, 2007, **515**, 3644-3652.

37. B. Podgornik, D. Hren, J. Vižintin, Low-friction behaviour of boundary lubricated diamond-like carbon coatings containing tungsten, *Thin Solid Films*, 2005, **476**, 92-100.

38. H. Spikes, The history and mechanisms of ZDDP, *Tribol. Lett.*, 2004, **17**, 469-489.